



# COMMON DC BUS CHARGING SYSTEM FOR ELECTRIC VEHICLES POWERED BY BATTERIES, FUEL CELLS, SOLAR, AND WIND

<sup>1</sup>G. Ramesh, <sup>2</sup>M. Ashmitha, <sup>3</sup>O. Poojitha, <sup>4</sup>K. Rathnesh, <sup>5</sup>P. Abhishek

<sup>1</sup>Assistant Professor, <sup>2,3,4,5</sup>UG Students

<sup>1,2,3,4,5</sup>Department of EEE

<sup>1,2,3,4,5</sup>Jyothishmathi Institute of Technology and Science, Nustulapur, Karimnagar, TS, India

**Abstract:** One potential solution to the growing need for electric vehicle charging stations is to set them up using renewable energy sources. Electric vehicle charging systems that use wind turbines, fuel cell stacks, and solar arrays often include a cascaded IIR filter and a five-level inverter. In the event that the grid goes down or becomes unavailable, control systems that rely on current and voltage can keep things running smoothly, thanks to static transfer switches. Modalities associated with grid presence and non-existence will consistently function with a cascaded IIR filter. In addition, even under very adverse grid circumstances, the system manages to work well. The energy riddle includes fuel cells, utility networks, power quality, distributed energy sources, fuel photovoltaic arrays, and solar photovoltaic arrays.

**IndexTerms - Power quality, distributed energy sources, solar photovoltaic array, fuel cell, wind turbine, five level inverter, utility grid, and cascading IIR filter**

## I. INTRODUCTION

There is a widespread belief that EVs will significantly reduce pollution from automobiles on the road. Strategies implemented on a global scale to encourage the use of EVs are also adding to the exponential growth in this sector. Electric vehicles, on the other hand, have a limited range, which means they need to be recharged often while driving [1]. The primary challenges to the widespread adoption of electric vehicles are their very high pricing and relatively limited battery lives. Concerns about the environment have sparked a flurry of research into the feasibility of mass-producing charging stations for electric vehicles, with a focus on those that run on renewable energy. So, power for EV charging stations is coming from renewable sources like solar panels, wind turbines, and fuel cell stacks. Energy economy, long working range, little exhausts pollution, and quiet operation are further reasons fuel cells are being used. Combustion is rendered obsolete by fuel cells, which electrochemically transform chemical energy into electrical energy. One promising option for a vehicle power source is the proton exchange membrane fuel cell, which has a low operating temperature and doesn't produce any harmful pollutants [2]. There is an effort to increase the use of wind power since it is plentiful, produces less waste, and is beneficial to the environment. However, the fact that the magnitude of the wind speed [3] changes hour to hour is a big drawback of using it. A hybrid strategy that takes into account the inherent uncertainty of any distributed energy source is necessary to satisfy the power demand while simultaneously improving environmental conditions. Using the correct management algorithms to charge electric automobiles is a major problem nowadays. When it comes to frequency mapping and ease of implementation, the second-order generalized integrator control approach is usually mentioned the most. Consequently, the SOGI [5] control approach makes it feasible to make the orthogonal signal generator. The processing time is reduced by integrator delays, but using them has the drawback of inter-harmonics. Furthermore, DC offset causes inaccurate estimate and decreases performance. In order to get a suitable steady-state outcome while being cognizant of the imminent switching state, the model predictive based control method is used, as shown in [6]. In dynamic situations, however, its ineffectiveness is made clear by the fact that adopting complicated structures increases processing complexity. The grid-connected operation uses a cascaded IIR filter to monitor the behaviour [7]. As mentioned in the IEEE519 standard, the cascaded IIR filter has better power quality and adequate performance, among other advantages. This arrangement describes the charging of electric vehicles (EVs) using a combination of a wind turbine, fuel cells, and photovoltaic (PV) arrays. The system complies with the IEEE-1547 standard for efficient power transmission and operates correctly in both connected and disconnected modes from the grid. Some major benefits that have resulted from this study are as follows.

In the event of grid availability issues or malfunction, this distributed generation system (DGS) may switch between island and grid-connected modes of operation.

The synchronization unit uses the phase angle estimator based on a cascaded IIR filter and full-lip-lock loop to enhance grid synchronization and protect it from voltage distortion and frequency variations.

Renewable energy sources, such as solar and wind, may now provide high-quality active powers to the grid via the grid-connected mode and the improved control algorithm. We have taken extra precautions to ensure that DC-offset and load current harmonics do not degrade the quality of the grid current.

The solar power feed-forward term enhances DGS's capacity to dynamically react to abrupt and significant changes in solar irradiation while operating in grid-connected mode. Power quality and reliability are enhanced in electric vehicle charging systems that include wind turbines, fuel cell stacks, and solar arrays.

When operated in grid existence mode, the cascaded IIR filter achieves adequate performance as per IEEE specifications. The DGS is designed to immediately transition to an isolated mode in the event of a grid failure, guaranteeing reliable operation and continuous service. With the help of the PI controller, the balanced and sinusoidal CCP (Common Coupling Point) voltages may be achieved when the DGS is operating in island mode. As a result, compared to the IEEE-1547 standard, the CCP voltage power quality is consistently superior.

## II. LITERATURE SURVEY

It is said in "Battery Energy Storage System (BESS) and Battery Management System (BMS) for Grid-Scale Applications" by M. T. Lawder that the current electric grid is inefficient and wastes a lot of electricity because there is a mismatch between consumer demand and generating capacity. In order to keep the power quality high enough, power plants often produce more energy than is really needed. The energy storage capacity of the system might be used as a potential remedy for these inefficiencies. Complex modeling is required for the proper regulation and monitoring of grid storage systems that use BESS. The functioning of the storage system may be regulated and its reliability guaranteed by a BMS using complex models based on physical principles. The current and future state of BMS modeling is highlighted in this paper so that vanadium and lithium-ion redox-flow batteries may make the most of BMS. In addition, we go over the system's design and how it may improve control and monitoring. We detail an approach to enhancing BMS that will allow it to use BESS more effectively for grid-scale applications. In their article titled "Robust Energy Management for Microgrids with High-Penetration Renewables," Y. Zhang, N. Gatsis, and G. B. Giannakis state that distributed energy management is essential for smart grids and microgrids that use DG and DS specifically. This is due to the fact that it decreases communication overhead and can withstand degradations. Within the framework of a microgrid that is heavily dependent on renewable energy sources and employs grid-connected demand-side management, this article delves into the idea of distributed economic dispatch. Given the unpredictability of RES availability, we provide a new approach to power scheduling. Through the integration of renewable energy sources with power traded with the main grid, this technique has the ability to stabilize the supply-and-demand balance. Considering the utility of dispatchable loads, the prices of DG and DS, and the worst-case transaction cost due to uncertainty in RES is the best approach to plan things in a manner that reduces the microgrid net cost. In order to decentralize the optimization problem, the DG, DS, and dispatchable load local controllers use dual decomposition. The effectiveness of the new approach is backed by quantitative data. G. He, Q. Chen, C. Kang, and Q. Xia's "Optimal Offering Strategy for Concentrating Solar Power Plants in Joint Energy, Reserve and Regulation Markets" suggests that thermal energy storage (TES) capable CSP plants may provide supplementary services (AS) in the reserve and regulatory markets. The increased revenue for CSP units and the general adaptability of electricity networks are two advantages of AS. While there is a wide range in solar power production, CSP installations would be far less adaptable with the improper strategy, such an excess of AS. A failure to adapt may lead to a precipitous decline in solar energy production and profitability. This research takes a look at the day-ahead energy, reserve, and regulatory markets to figure out how CSP facilities can make the most money. The model is robust against both the unpredictability of solar energy and the volatility of market prices. Based on the best day-ahead offering strategy, we may calculate the opportunity cost and use it to create offering curves for supplemental AS markets that provide extra AS capabilities. Using the updated maximum permissible curtailment rate index, CSP facilities may weigh the pros and cons of AS supply and solar energy accommodation flexibility. That the proposed paradigm is sound was shown by the case study.

In their study titled "Grid integration of three-phase single-stage PV system using adaptive laguerre filter based control algorithm under non-ideal distribution system," P. Shukl and B. Singh present a grid-connected, one-stage solar PV (photovoltaic) system. One approach that could maximize the efficiency of solar arrays is Maximum Power Point Tracking, which is based on the P&O methodology. A method based on adaptive Laguerre filters is used to regulate the voltage source converter. To keep the DC link voltage relative to the reference value, a PI (Proportional Integral) controller may be used. The operation of the grid-connected PV system may be studied by subjecting a functional model to a series of controlled tests. We show that the system can withstand a wide variety of loads under less-than-ideal conditions.

Keeping the power quality constant in the distribution network is becoming more difficult due to the growing number of power electronics converters used in households, companies, and industries, as stated in "Power Quality: Problems and Mitigation Techniques" by B. Singh, Chandra, and K. Al-Hadad. Increased losses, underutilized distribution systems, and the malfunction of sensitive equipment are the knock-on effects of declining power quality on surrounding consumers, protective devices, and communication systems. Because of the energy savings benefits, power electronics converters will handle more alternating current (AC) power; hence, we must promptly resolve power quality issues.



### III. EXISTING SYSTEM

Figure 1 depicts the system architecture that allows for the extensive use of distributed energy sources such as solar PV arrays, wind turbines, batteries, and fuel cell stacks for DC bus-based electric vehicle charging. The utility grid is connected to the hybrid renewable power sources via a central converter and backup batteries. Electric vehicles may be charged at STSs, and grid participation and disengagement can also be facilitated. Using incremental conductance based maximum power point tracking (MPPT) algorithms, the switching pulses (Spv, Sfc) of the appropriate boost converters are derived from the maximum powers of the solar PV arrays and PEM fuel cell stacks.

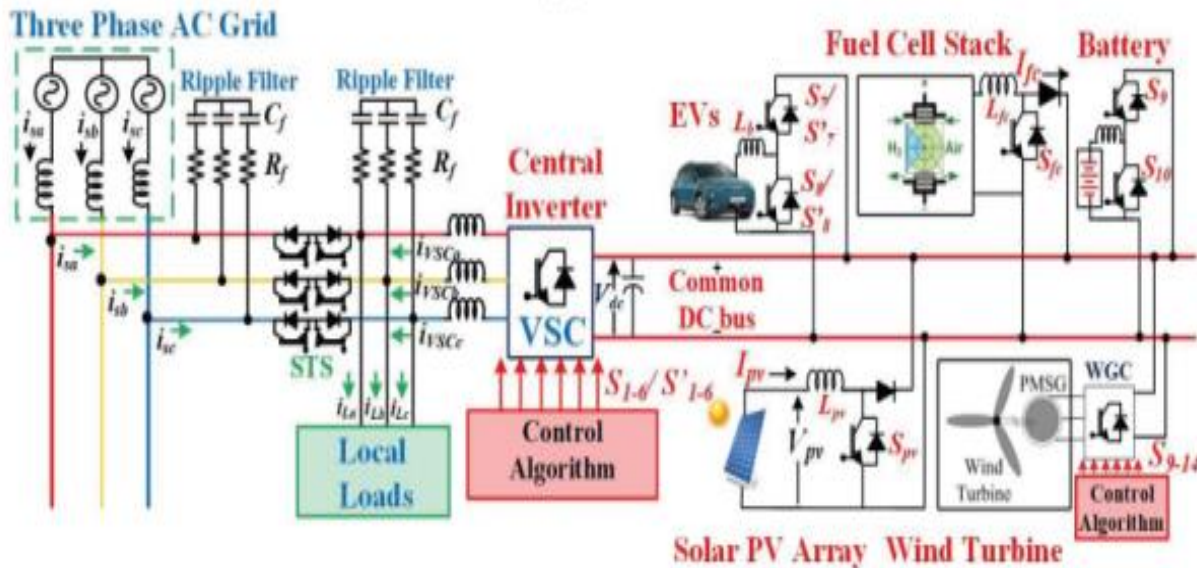


Figure 1: Distributed microgrid based EVs charging infrastructure

### IV. PROPOSED SYSTEM

The DC bus charging system design for electric vehicles (EVs) is shown in Figure 2. It incorporates distributed energy sources such as wind turbines, batteries, fuel cell stacks, solar photovoltaic (PV) arrays, and so on. To connect the hybrid renewable power sources to the power grid, a battery and a central inverter—also called a five-level inverter—are used. At STSs, you may charge your electric car and either participate in or disconnect from the grid. From the maximum powers of the solar PV arrays and PEM fuel cell stacks, the switching pulses (Spv, Sfc) of the relevant boost converters are calculated using incremental conductance based maximum power point tracking (MPPT) algorithms. After that, a fully-controlled AC-DC converter connects the wind turbine to a wind power generating converter, which is also called a permanent magnet synchronous generator (PMSG).

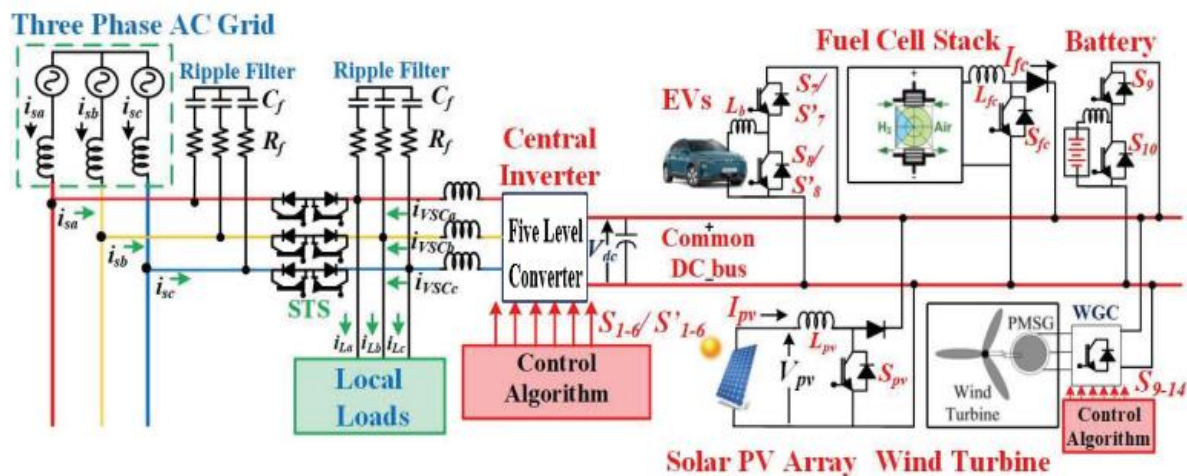


Figure 2: Proposed system along with five level inverter

### V. CONTROL METHODOLOGY RESULTS

Here are several ways to manage the distributed microgrid, which is a typical configuration for DC bus charging EVs. A voltage control is used for management when the system is connected to the grid. A control method based on cascading IIR filters is used to decrease harmonics when it is off-grid. The grid line voltages (vsab, vsbc) are used to get the grid phase voltages [8],

$$v_{sa} = \frac{v_{sbc}}{3} + \frac{2v_{sab}}{3}, v_{sb} = \frac{v_{sbc}}{3} - \frac{v_{sab}}{3}, v_{sc} = \frac{2v_{sbc}}{3} - \frac{v_{sab}}{3} \quad (1)$$

Consequently, the terminal voltage ( $V_t$ ) is calculated by using the acquired grid phase voltages ( $v_{sa}$ ,  $v_{sb}$ ,  $v_{sc}$ ) in the following way:

$$v_t = \sqrt{2(v_{sa}^2 + v_{sb}^2 + v_{sc}^2)/3} \tag{2}$$

Here are the techniques to use the  $v_{sa}$ ,  $v_{sb}$ ,  $v_{sc}$ , and  $V_t$  to get  $u_{qa}$ ,  $u_{qb}$ , and  $u_{qc}$ :

$$u_{pa} = v_{sa}/V_t, u_{pb} = v_{sb}/V_t, u_{pc} = v_{sc}/V_t \tag{3}$$

$$u_{pa} = \frac{-u_{pb}}{\sqrt{3}} + \frac{u_{pb}}{\sqrt{3}}, u_{qb} = \frac{3u_{pa}}{2\sqrt{3}} + \frac{u_{pb}}{2\sqrt{3}} - \frac{u_{pc}}{2\sqrt{3}}, u_{qc} = \frac{-3u_{pa}}{2\sqrt{3}} + \frac{u_{pb}}{2\sqrt{3}} - \frac{u_{pc}}{2\sqrt{3}} \tag{4}$$

In grid-connected mode of operation, cascading IIR filters precisely predict the active power component of the load, enabling proper VSC switching. The transfer function is shown here:

$$\frac{i_{Lfa}}{i_{La}} = \frac{[-k_1z^{-1}\alpha_2 + (-h_1k_1z^{-2})][-k_1z^{-1}\alpha_1 + (-h_0k_1z^{-2})]}{(1-\alpha_2z^{-1})(1-\alpha_1z^{-1})} \tag{5}$$

So,  $i_{Lfa}$ , the fundamental element, is harmonic-free and has a sinusoidal waveform. The  $i_{Lfa}$  attained serves as a companion to the quadrature phase unit templates. As a consequence,  $I_{fpa}$  is bought after ascertaining  $I_{fpb}$  and  $I_{fpc}$  by computation using absolute blocks. We predict that the  $I_{pLavg}$  will be

$$I_{pLavg} = \frac{I_{fpa} + I_{fpb} + I_{fpc}}{3} \tag{6}$$

In addition, it is necessary to acquire the voltage error ( $V_{eve}$ ) using the EVs'  $V_{ev}$  and  $V_{ev}^*$  in order to allow EV charging:

$$V_{eve} = V_{ev}^* - V_{ev} \tag{7}$$

Here is how the reference current ( $I_{ev}^*$ ) of the EVs is calculated using the output voltage error ( $V_{eve}$ ):

$$I_{ev}^*(m) = I_{ev}^*(m-1) + K_{pev}\{V_{eve}(m)\} + K_{iev}\{V_{eve}(m) - V_{eve}(m-1)\} \tag{8}$$

When the reference and measured currents of the electric cars are compared, a current error is determined, as

$$I_{eve} = I_{ev}^* - I_{ev} \tag{9}$$

$D_{eve}$  is used to calculate the pulses for the S7-S8 bidirectional converter in EVs.

$$D_{eve} = D_{eve}(m-1) + K_{peve}\{I_{eve}(m)\} + K_{ieve}\{I_{eve}(m) - I_{eve}(m-1)\} \tag{10}$$

Furthermore, for battery control, the voltage error is computed by means of

$$V_{dce} = V_{dc}^* - V_{dc} \tag{11}$$

To get the battery reference current, one uses the voltage error in this way:

$$I_{batt}^*(m) = I_{batt}^*(m-1) + K_{pdcb}\{V_{dce}(m)\} + K_{idcb}\{V_{dce}(m) - V_{dce}(m-1)\} \tag{12}$$

Therefore, by comparing the battery's reference current with the current we sense in the battery ( $I_{batt}$ ), we may estimate the current error as

$$I_{battr} = I_{batt}^* - I_{batt} \tag{13}$$

Batteries with bidirectional converters are expected to have switching pulses that are

$$D = D(m-1) + K_{pbatt}\{I_{batt}(m)\} + K_{ibatt}\{I_{batt}(m) - I_{batt}(m-1)\} \tag{14}$$

Furthermore, the wind turbine-powered PMSG is controlled using vectors, and the estimated  $I_q^*$  is

$$I_q^*(k) = I_q^*(k-1) + K_{pww}\{\omega_{error}(k)\} + K_{iww}\{\omega_{error}(k) - \omega_{error}(k-1)\} \tag{15}$$

The PI speed controller's gains are denoted by  $k_{pw}$  and  $k_{iw}$ , while the discrepancy between the reference and observed rotor speeds is represented by the value of  $\omega_{error}$ . An incremental conductance-based MPPT control approach is used to

determine the reference rotor speed.  $I^* d$  and  $I^* q$  are used to round off  $I^* g_{ena}$ ,  $i^* g_{enb}$ , and  $i^* g_{enc}$ , respectively. The ensuing pulses (S9-S14) of the WGC switching are shown in Figure 2. Wind turbine, fuel cell stack, and PV array work together as seen in Fig. 3 to extract the most electricity possible. Future feed-forward terms for the wind turbine, fuel cell stack, and solar array are expected to include,

$$\omega_{pv} = \frac{2P_{pv}}{3V_t}, \omega_{fc} = \frac{2P_{fc}}{3V_t}, \omega_{wind} = \frac{2P_w}{3V_t} \quad (16)$$

Pv, Pfc, Vt, and Pw stand for voltage at the terminal, power from a wind turbine, combined with power from a PV fuel cell stack. Applications such as  $I_{pLav}$ ,  $w_{pv}$ ,  $w_{fc}$ ,  $w_{wind}$ , and  $w_{batt}$  are used for the purpose of assessing an IP network.

$$I_{pnet} = I_{pLav} - (w_{pv} + w_{fc} + w_{wind} + w_{ev} + w_{batt}) \quad (17)$$

The electric vehicle contribution ( $w_{ev}$ ) and the battery contribution ( $w_{batt}$ ) are calculated as  $(2P_{ev} / 3V_t)$  and  $(2P_{batt} / 3V_t)$ , respectively. By multiplying  $I_{pnet}$  with  $u_{pa}$ ,  $u_{pb}$ , and  $u_{pc}$ , we get as

$$i^*_{sa} = I_{pnet} * u_{pa}, i^*_{sb} = I_{pnet} * u_{pb}, i^*_{sc} = I_{pnet} * u_{pa} \quad (18)$$

In order to determine the switching pulses (S1-S6) of VSC, we input the current errors into the hysteresis current controller. When the grid is not in use, the following assessments of  $v^*_{La}$ ,  $v^*_{Lb}$ , and  $v^*_{Lc}$  are carried out, supposing STS=0:

$$v^*_{La} = v_{ref} * \sin\theta_m, v^*_{Lb} = v_{ref} * \sin(\theta_m - 120^\circ), v^*_{Lc} = v_{ref} * \sin(\theta_m - 240^\circ) \quad (19)$$

The load voltage angle, denoted as  $\theta_m$ , and the amplitude of the load voltages, denoted as  $V_{ref}$ , are calculated from the three-phase load voltages. The following is how the reference load currents ( $i^*_{La1}$ ,  $i^*_{Lb1}$ ,  $i^*_{Lc1}$ ) are generated by the PR controller [9] using the voltage error that is determined from the sensor and reference load voltages:

$$i^*_{La} = T_a(s) * v_{Lae}(s) = \left\{ k_{pae} + \frac{(k_{iae}2\omega_c s)}{(s^2 + 2\omega_c s + \omega_c^2)} \right\} * v_{Lae}(s) \quad (20)$$

$$i^*_{Lb} = T_a(s) * v_{Lbe}(s) = \left\{ k_{pbe} + \frac{(k_{ibe}2\omega_c s)}{(s^2 + 2\omega_c s + \omega_c^2)} \right\} * v_{Lbe}(s) \quad (21)$$

$$i^*_{Lc} = T_a(s) * v_{Lce}(s) = \left\{ k_{pce} + \frac{(k_{ice}2\omega_c s)}{(s^2 + 2\omega_c s + \omega_c^2)} \right\} * v_{Lce}(s) \quad (22)$$

Therefore,  $i_{eLa}$ ,  $i_{eLb}$ , and  $i_{eLc}$  are used to estimate S' 1-S' 6.

$$i_{eLa} = i^*_{La} - i_{La}, i_{eLb} = i^*_{Lb} - i_{Lb}, i_{eLc} = i^*_{Lc} - i_{Lc} \quad (23)$$

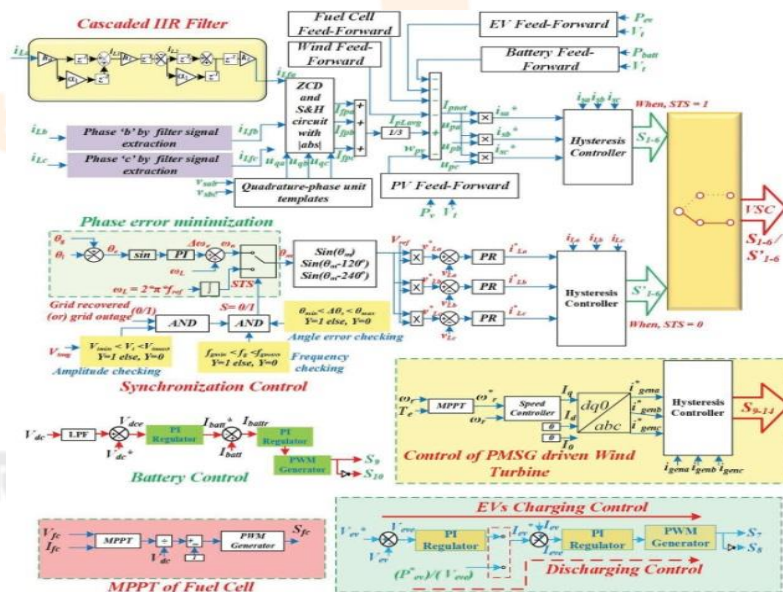


Figure 3

Taking charge of a decentralized microgrid that draws power from renewable resources like solar panels, wind turbines, batteries, and fuel cells, whether they're linked to the grid or not Possible ways to coordinate distributed microgrids with shared DC bus charging for electric vehicles consisting of fuel cell, solar, wind and battery sources is also shown in Fig. 2.

For reconnection to the power grid, the independent system's voltages and phase angles are synchronized with the power grid's. Finding the phase angles is the first step in using a PI controller to bring them into harmony. Because of this, we can calculate the phase inaccuracy as

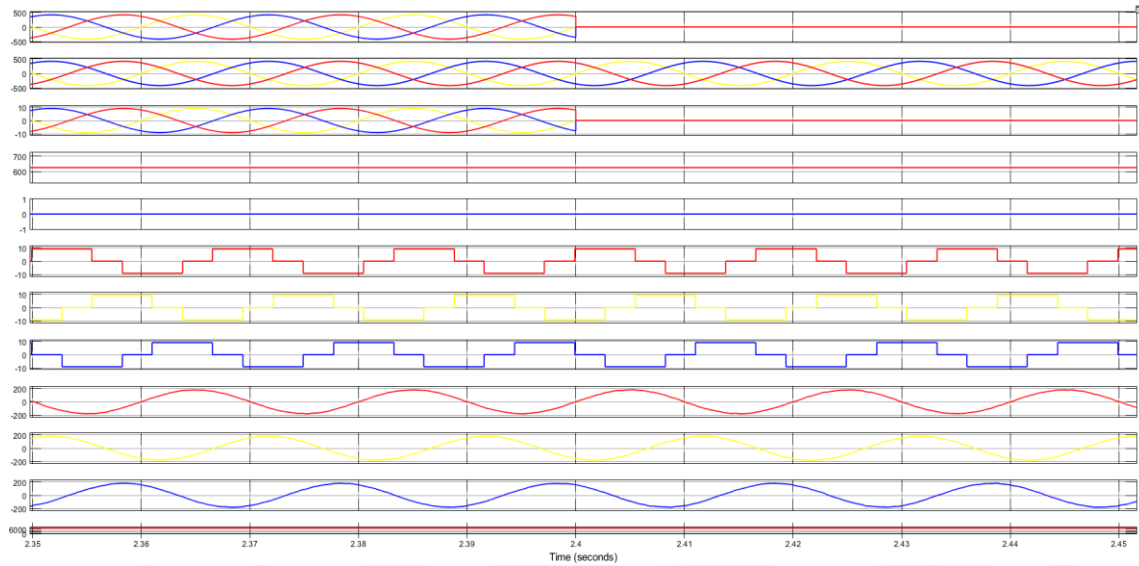
$$\theta_e = \theta_g - \theta_L \quad (24)$$

$$\Delta\omega_c(n) = \Delta\omega_c(n - 1) + k_{pc}\{\theta_{c_c}(n) - \theta_{c_c}(n - 1)\} + k_{ie}\theta_{c_c}(n) \tag{25}$$

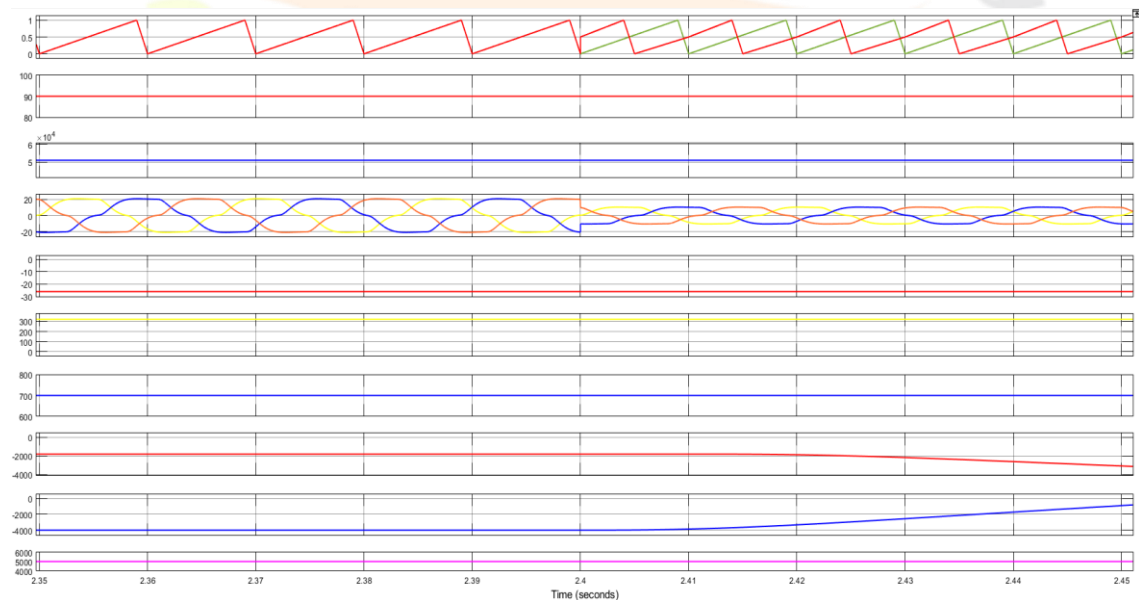
When trying to estimate frequency inaccuracy, the PI controller comes in handy, because the frequency shift, shown by  $\Delta\omega_c$ , is essential for maintaining synchronization with the main grid.  $\check{C}n = (\Delta\check{v}e + \check{v}L)$  is used to estimate the new frequency during grid retrieval. The load's fundamental frequency ( $\check{v}L$ ) is the only signal sent while operating independently.

## VI. SIMULATION RESULTS

### A) EXISTING RESULTS(THREE LEVEL INVERTER)



(a)



(b)



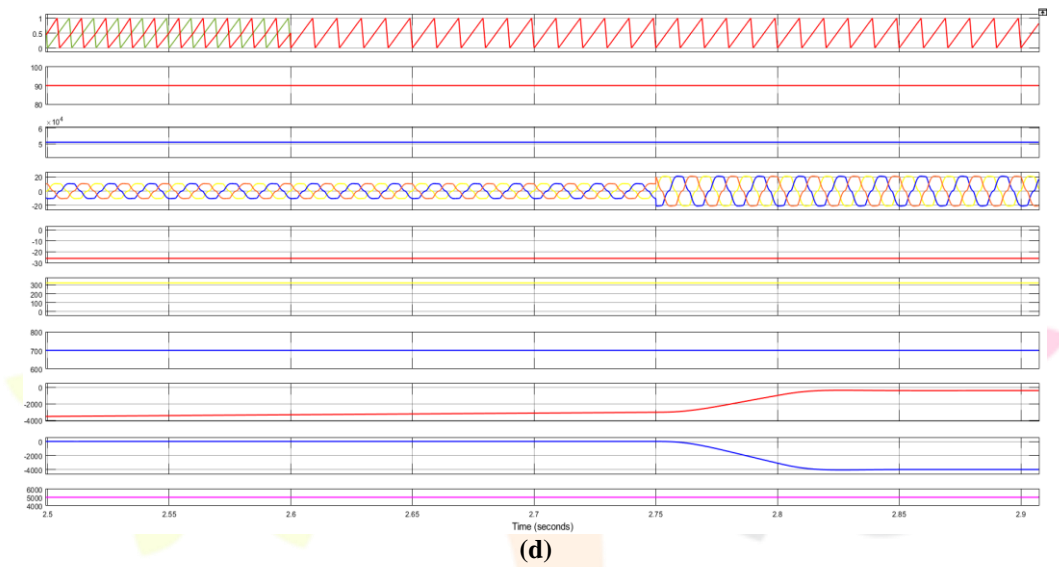
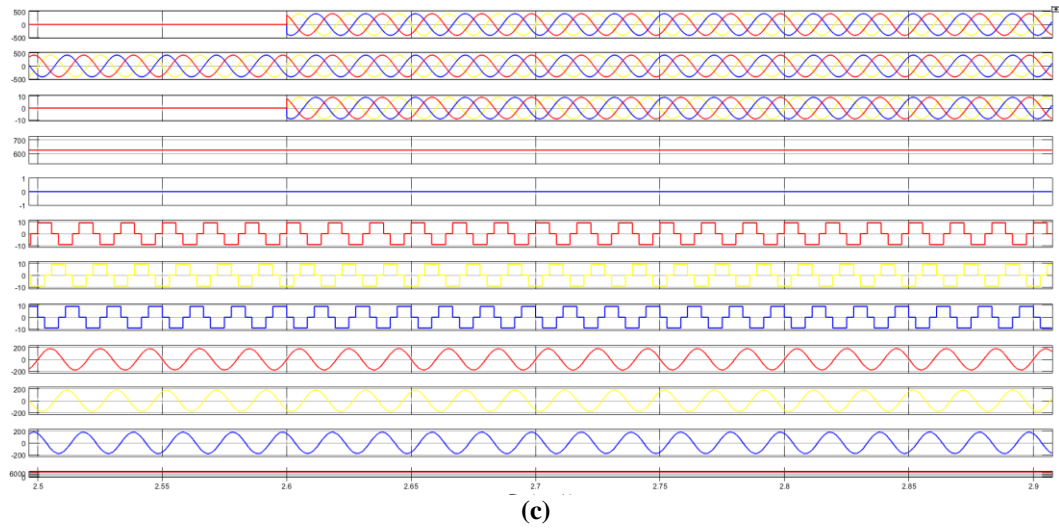
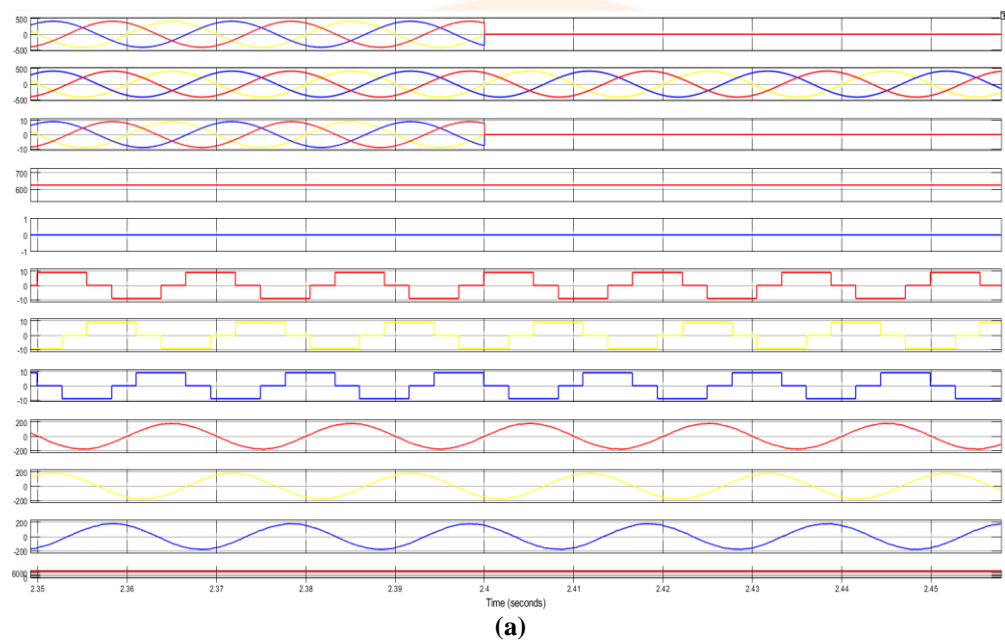
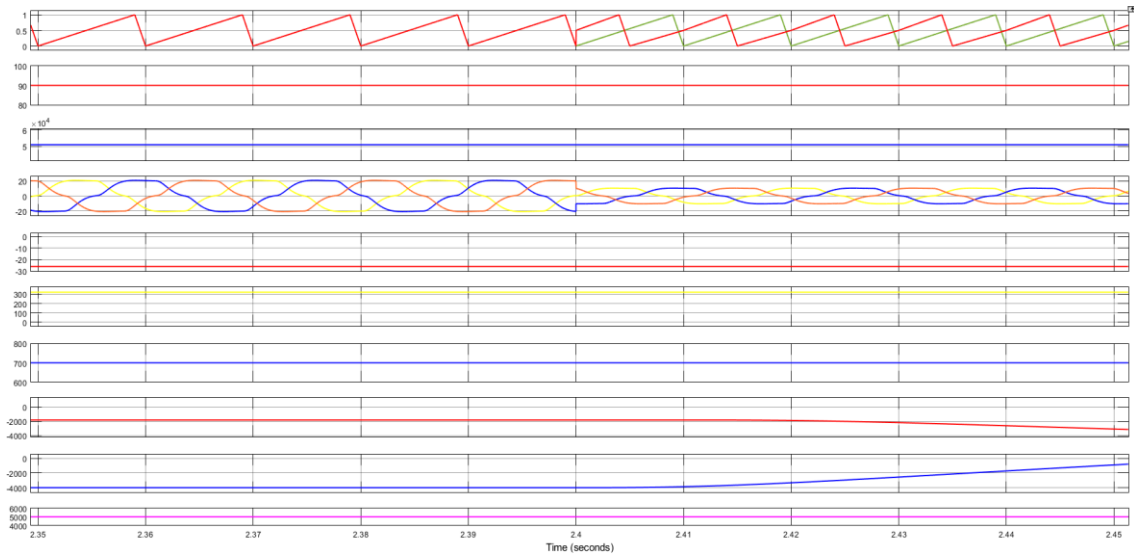
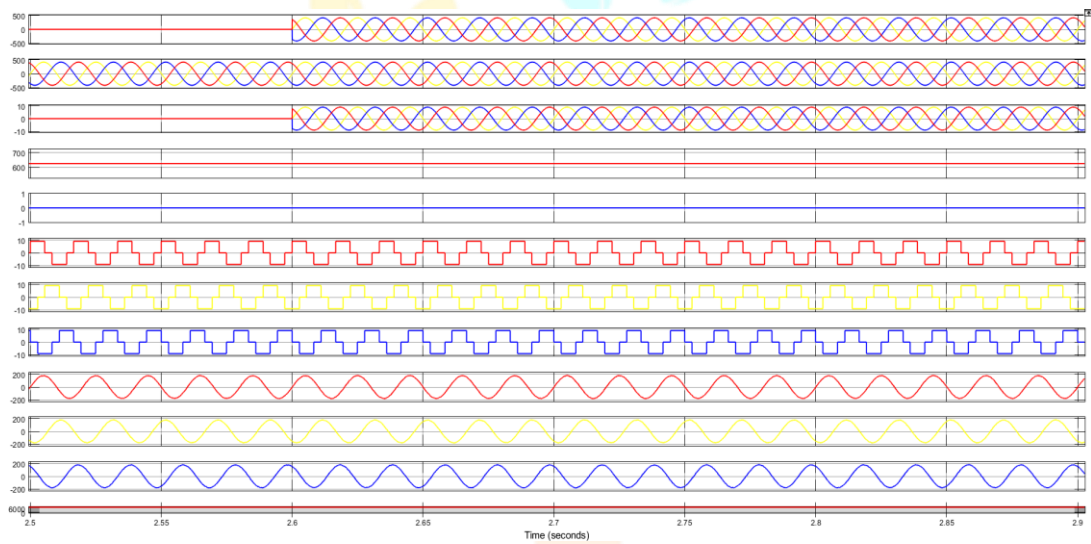


Figure 4: Simulated performance through transition between grid existence to non-existence operation

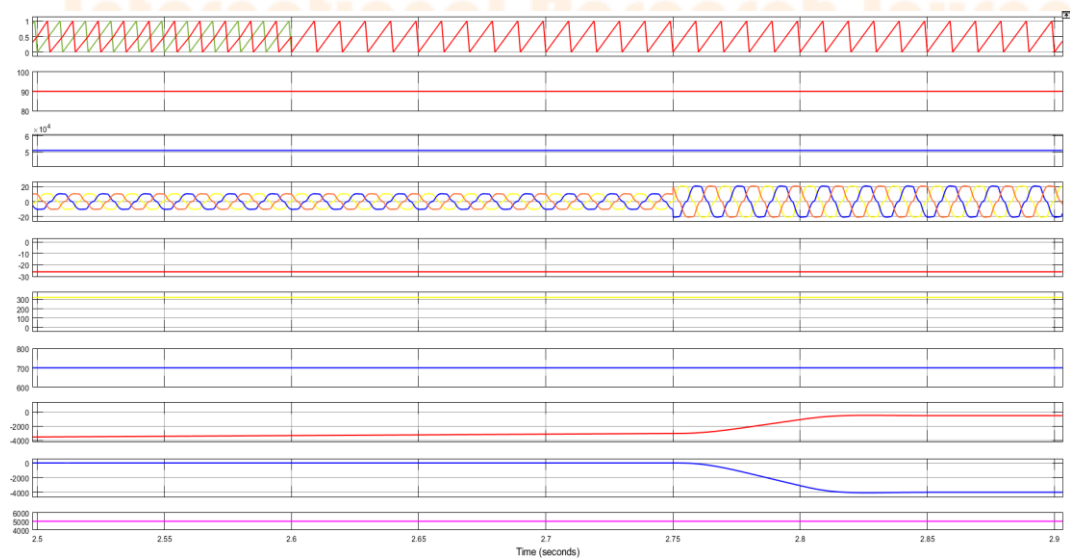




(b)



(c)

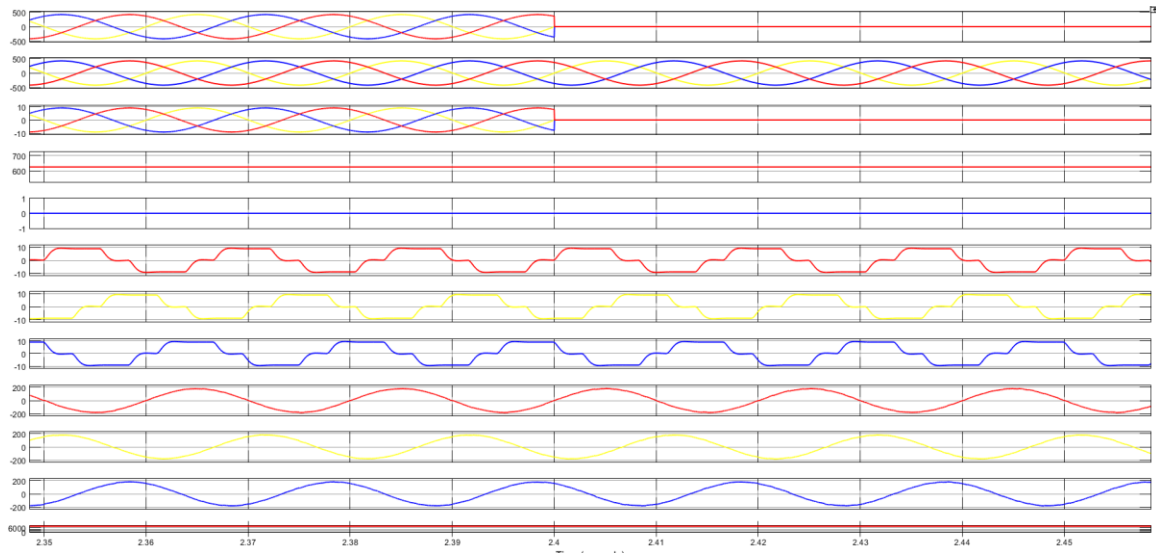


(d)

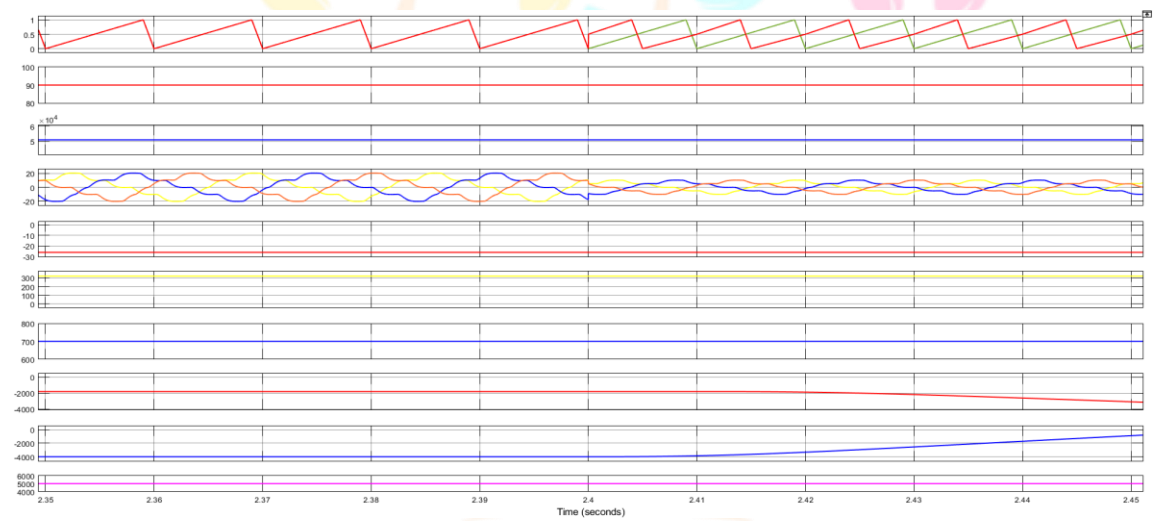
Figure. 5 Simulated performance during wind speed and solar insolation variation operation



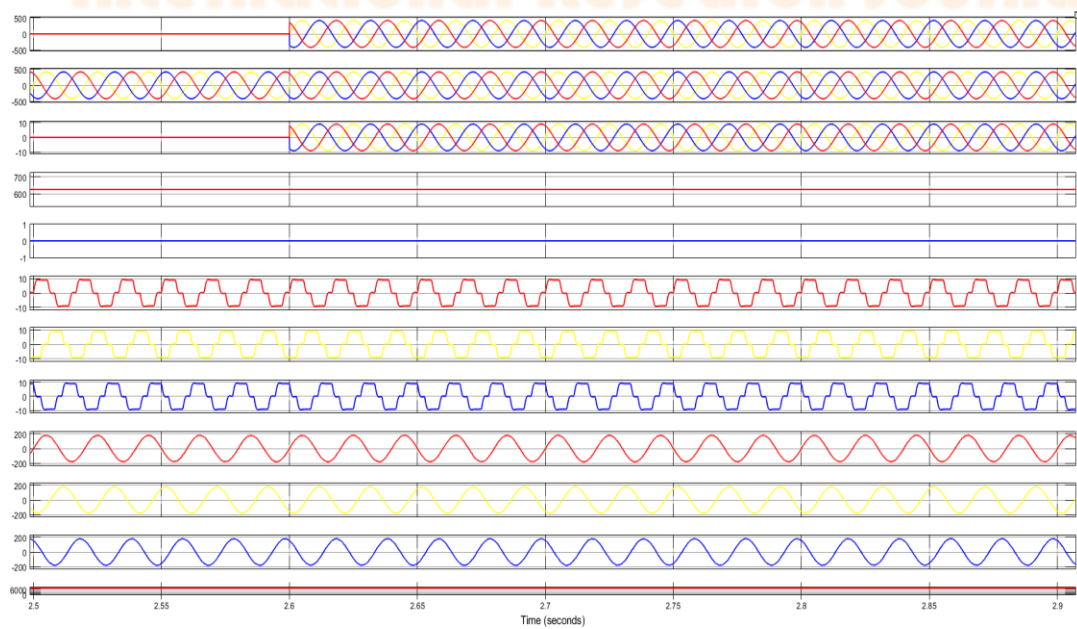
### B)EXTENSION RESULTS (FIVE LEVEL INVERTER)



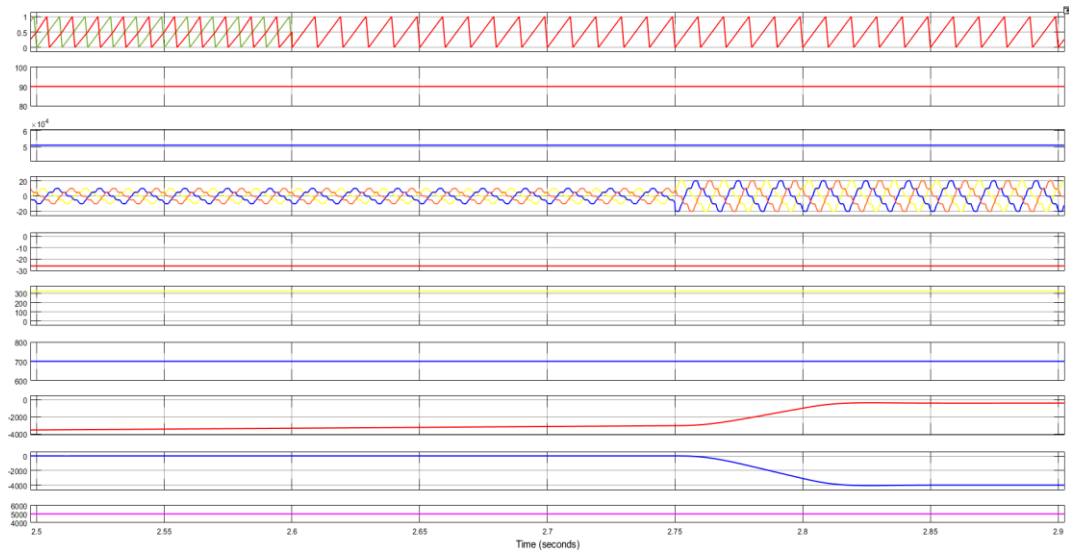
(a)



(b)

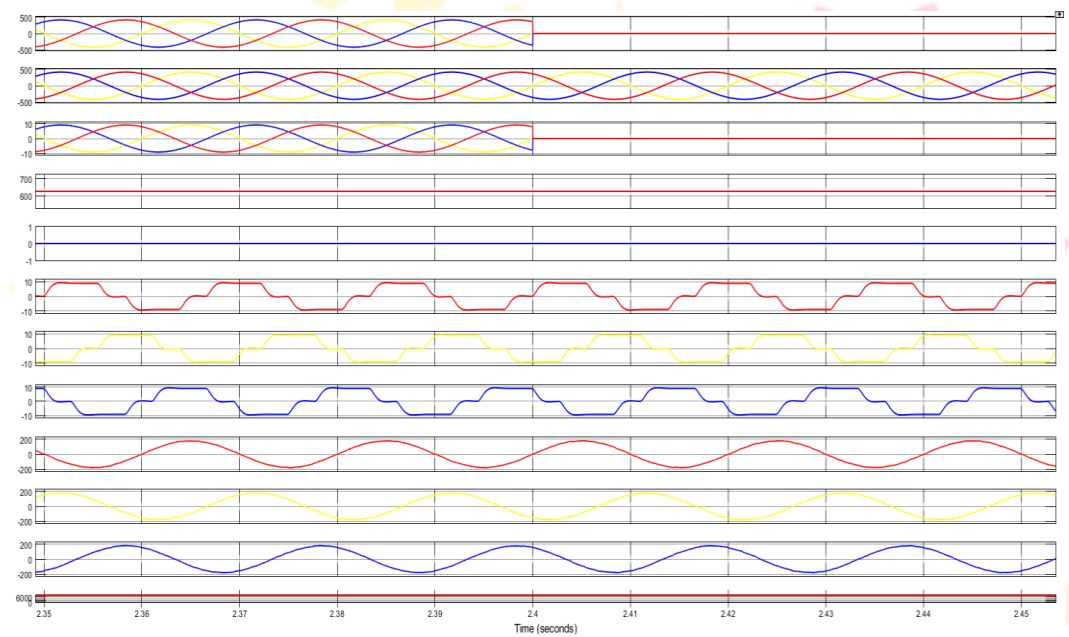


(c)

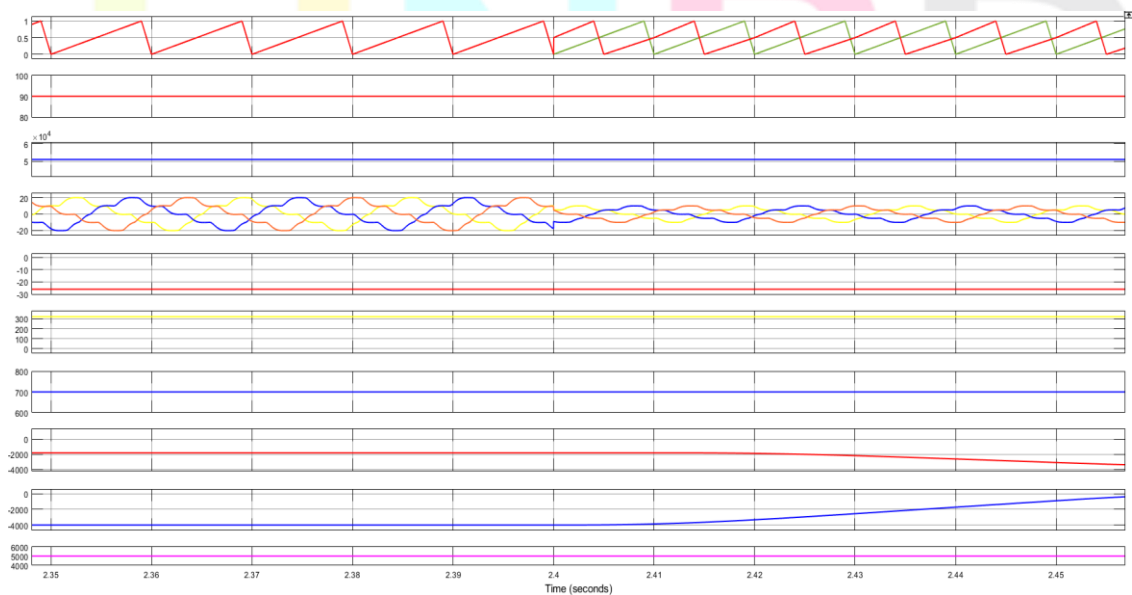


(d)

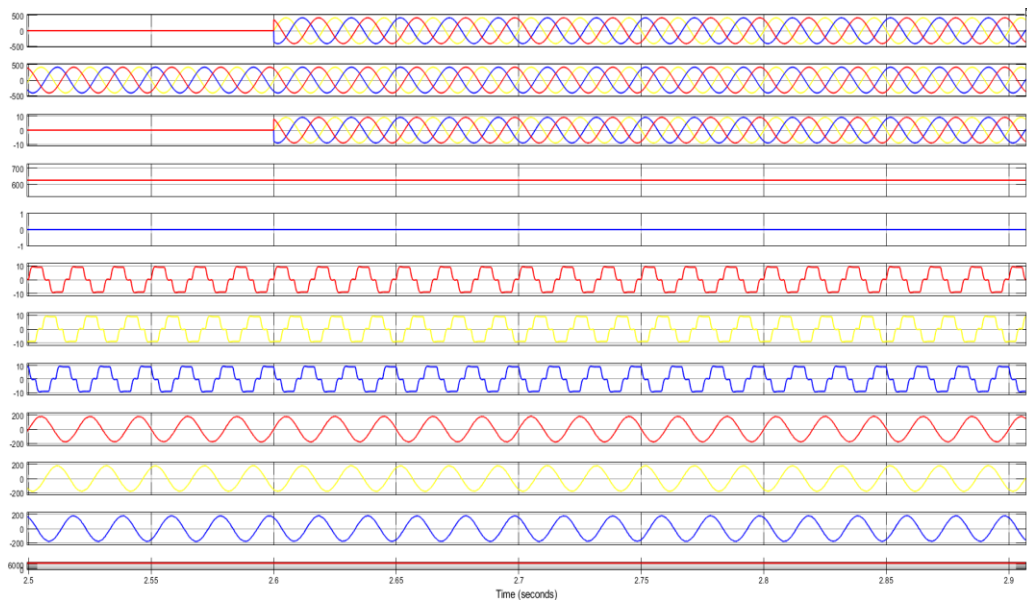
Figure.6 Simulated performance through transition between grid existence to non-existence operation



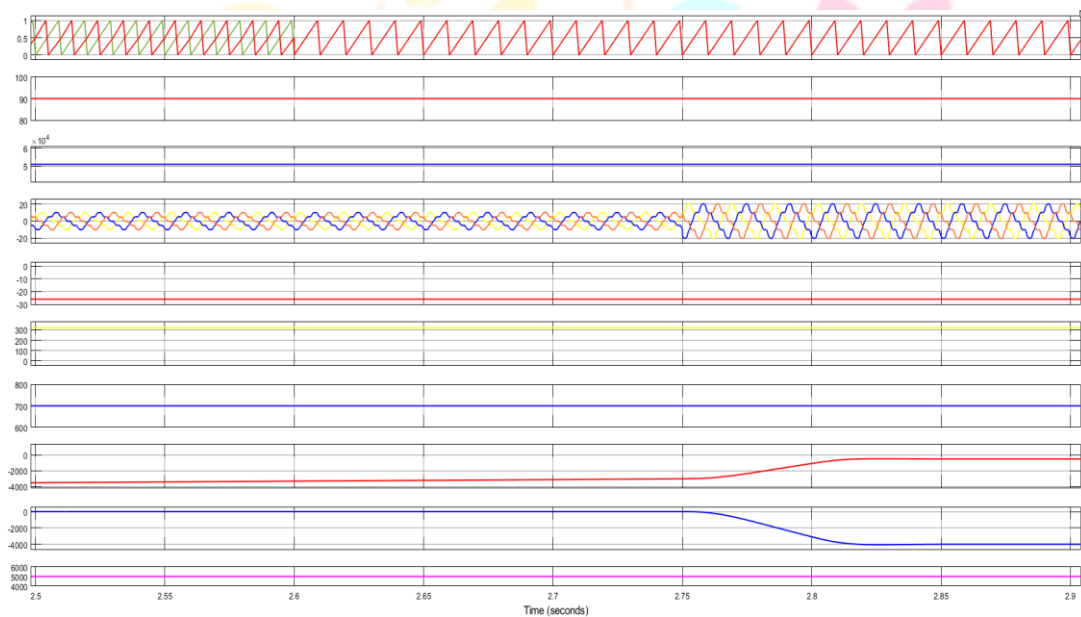
(a)



(b)



(c)



(d)

Figure.7 Simulated performance during wind speed and solar insolation variation operation

#### ACKNOWLEDGEMENT AND FUNDING

The authors receive no financial support for the research, authorship, and publication of this article.

#### DECLARATION OF CONFLICTING INTERESTS

The authors declare no potential conflicts of interest with respect to the research and publication of this article.

#### REFERENCES

- [1] Y. -T. Liao and C. -N. Lu. 2015. Dispatch of EV Charging Station Energy Resources for Sustainable Mobility. *IEEE Trans. Trans. Electrific.* 1(1):86-93.
- [2] G. Su and L. Tang. 2008. A Multiphase, Modular, Bidirectional, Triple Voltage DC–DC Converter for Hybrid and Fuel Cell Vehicle Power Systems. *IEEE Trans. Pow. Electr.* 23(6):3035-3046.
- [3] Q. Huang, Q. -S. Jia, Z. Qiu, X. Guan and G. Deconinck. 2015. Matching EV Charging Load With Uncertain Wind: A Simulation-Based Policy Improvement Approach. *IEEE Trans. Smart Grid.* 6(3):1425-1433.
- [4] C. Liu, K. T. Chau, D. Wu and S. Gao. 2013. Opportunities and Challenges of Vehicle-to-Home, Vehicle-to-Vehicle, and Vehicle-to-Grid Technologies. *Proceedings of the IEEE.* 101(11):2409-2427.
- [5] J. Matas, H. Martín, J. de la Hoz, A. Abusorrah, Y. A. Al-Turki and M. Al-Hindawi. 2018. A Family of Gradient Descent Grid Frequency Estimators for the SOGI Filter. *IEEE Trans. Pow. Electr.* 33(7):5796-5810.

- [6] M. B. Shadmand, R. S. Balog and H. Abu-Rub. 2014. Model Predictive Control of PV Sources in a Smart DC Distribution System: Maximum Power Point Tracking and Droop Control. IEEE Trans. Ener. Conv. 19(4):913-921.
- [7] N. Onizawa, S. Klosehita, S. Sakamoto, M. Kawamata and T. Hanyu. Evaluation of Stochastic Cascaded IIR Filters. Proc. IEEE International Symp. Multiple-Valued Logic. Pp:224-229.
- [8] B. Singh, Chandra, and K. Al-Hadad. 2015. Power Quality: Problems and Mitigation Techniques. John Wiley & Sons Ltd. U. K.
- [9] A. Kuperman. 2015. Proportional-Resonant Current Controllers Design Based on Desired Transient Performance. IEEE Trans. Pow. Electr. 33(10):5341-5345.

